

## Heavy-light susceptibilities in a strongly coupled quark-gluon plasma

Shuai Y. F. Liu <sup>1,2,3,4</sup> and Ralf Rapp <sup>3</sup>

<sup>1</sup>*School of Physics and Electronics, Hunan University, Changsha 410082, China*

<sup>2</sup>*Human Provincial Key Laboratory of High-Energy Scale Physics and Applications, Hunan University, Changsha 410082, China*

<sup>3</sup>*Cyclotron Institute and Department of Physics and Astronomy, Texas A&M University, College Station, Texas 77843-3366, USA*

<sup>4</sup>*Quark Matter Research Center, Institute of Modern Physics, Chinese Academy of Sciences, Lanzhou 730000, China*



(Received 19 April 2022; accepted 23 September 2022; published 18 November 2022)

Quark number susceptibilities as computed in lattice QCD are commonly believed to provide insights into the microscopic structure of QCD matter, in particular its degrees of freedom. We generalize a previously constructed partonic  $T$ -matrix approach to finite chemical potential to calculate various susceptibilities, in particular for configurations containing a heavy charm quark. At vanishing chemical potential and moderate temperatures, this approach predicts large collisional widths of partons generated by dynamically formed hadronic resonance states which lead to transport parameters characteristic for a strongly coupled system. The quark chemical potential dependence is implemented into the propagators and the in-medium color potential, where two newly introduced parameters for the thermal and screening masses are fixed through a fit to the baryon number susceptibility,  $\chi_2^B$ . With this setup, we calculate heavy-light susceptibilities without further tuning; the results qualitatively agree with the lattice-QCD (lQCD) data for both  $\chi_{11}^{uc}$  and  $\chi_{22}^{uc}$ . This implies that the lQCD results are compatible with a significant content of broad  $D$ -meson and charm-light diquark bound states in a moderately hot quark-gluon plasma.

DOI: [10.1103/PhysRevC.106.055201](https://doi.org/10.1103/PhysRevC.106.055201)

### I. INTRODUCTION

In ultrarelativistic heavy-ion collisions, a new state of matter—quark-gluon plasma (QGP)—can be created, at temperatures of almost  $10^9$  times the surface temperature of the sun, rendering the nuclear fireballs the hottest matter created in the laboratory to date. The QGP is a fundamental realization of a many-body system governed by the strong nuclear force described by quantum chromodynamics (QCD). Its properties, as deduced from heavy-ion collision experiments to date [1–4], suggest it to be a strongly coupled liquid with transport properties near conjectured lower bounds set by quantum mechanics. From the theoretical side, first-principle information can be obtained from numerical simulations of the space-time discretized partition function of QCD at finite temperature, referred to as lattice QCD. At vanishing baryon chemical potential,  $\mu_B = 0$ , lattice-QCD (lQCD) computations have achieved accurate results for the equation of state (EoS) of QCD matter [5,6] and revealed that the transition between hadronic matter and the QGP is a smooth crossover [7]. However, there are several quantities that are currently not accessible to lQCD computations and are not straightforward to extract from euclidean space-time. Nevertheless, high-quality

lQCD “data” provide valuable benchmarks and insights for microscopic model calculations that, in turn, can be deployed to the phenomenology of heavy-ion collisions.

The strategy of utilizing lQCD data as “numerical experimental data” for model building has been widely applied in the literature, including calculations of the EoS [8–10], quarkonium correlation functions [11–16], and/or heavy-quark (HQ) free energies [17,18]. Taking advantage of the progress in lQCD [5,6,19–22], we have developed a thermodynamic  $T$ -matrix approach [23,24] which is rooted in three sets of lQCD data: the HQ free energy, Euclidean quarkonium correlator ratios, and the EoS for  $N_f = 2 + 1$  light-quark flavors. The lQCD results were instrumental in constraining the input parameters for the  $T$ -matrix approach, in particular its in-medium driving kernel and the effective thermal-parton masses, and subsequently enabled controlled studies of spectral and transport properties of the QGP [23,25,26].

In addition, quark-number susceptibilities [27–30]—derivatives of the partition function with respect to chemical potentials of different quantum numbers such as baryon number, isospin, and/or strangeness—have proved to be a rich source of information for effective models (see, e.g., Ref. [31] for a recent review). They can probe aspects of the chiral transition, the EoS (e.g., its hadron-chemistry and extension to finite  $\mu_B$ ), and its fluctuation properties, related to the effective degrees of freedom of the charge carriers. In the present paper, we are mostly interested in the latter aspect in the context of the thermodynamic  $T$ -matrix approach mentioned above. For moderate QGP temperatures, it predicts the emergence of broad hadronic bound states whose role in the EoS gradually increases as the pseudocritical temperature ( $T_{pc}$ ) is approached

Published by the American Physical Society under the terms of the [Creative Commons Attribution 4.0 International](https://creativecommons.org/licenses/by/4.0/) license. Further distribution of this work must maintain attribution to the author(s) and the published article’s title, journal citation, and DOI. Funded by SCOAP<sup>3</sup>.

from above. These states, which are generated from a ladder resummation of the in-medium interaction kernel, play a key role in producing large (resonant) interaction strength for elastic parton scattering, which entails transport parameters characteristic for a strongly coupled system [23]. The diagonal charm-quark susceptibility,  $\chi_2^c$ , was calculated previously in the  $T$ -matrix approach in Ref. [16], where the free and internal energies were used as potential proxies. In particular, it was found that sizable charm-quark widths,  $\Gamma_c \simeq 100\text{--}200$  MeV, can lead to a significant enhancement over the zero-width quasiparticle result.

Besides the diagonal susceptibilities,  $\chi_{2,4}^c$ , IQCD computations are also available for off-diagonal heavy-light combinations,  $\chi_{11}^{uc}$  and  $\chi_{22}^{uc}$  [32,33]. Model calculations have thus far focused on off-diagonal susceptibilities in the  $N_f = 2 + 1$  sector, i.e.,  $\chi_{11}^{us}$  or  $\chi_{11}^{ud}$ . In perturbative hard-thermal loop (HTL) calculations [34], the latter have been found to vanish, but they are expected to become nonvanishing at order  $g^6$  (including an additional logarithmic dependence) [35]. Within Polyakov loop-extended Nambu–Jona-Lasinio (PNJL) models [36,37] and the hadron resonance gas (HRG) model [38,39],  $\chi_{11}^{us}$  has been found to be negative, in agreement with IQCD data, indicating the importance of hadronic degrees of freedom in the vicinity of  $T_{pc}$ . The analysis of the off-diagonal heavy-light susceptibilities from IQCD [32,33] using a schematic model of a mixture of HRG and free charm-quark degrees of freedom suggest a similar interpretation in the charm sector. The formation of heavy-light resonance states in the QGP has been put forward in earlier works [25,40–42] as a key ingredient to evaluate the HQ diffusion coefficient, which requires a large nonperturbative contribution in order to describe open heavy-flavor observables in heavy-ion collisions [43,44]. It is therefore important to investigate the manifestation of heavy-light correlations in the off-diagonal heavy-light susceptibilities for which very few calculations are available to date [39]. In particular, we are not aware of a strongly coupled approach beyond mean-field approximations. In the present study we employ the  $T$ -matrix approach, which realizes a strong-coupling scenario through the dynamical formation of hadronic states as the QGP temperature decreases toward  $T_{pc}$ .

The remainder of the paper is organized as follows. In Sec. II, we briefly recall the basic components of the  $T$ -matrix formalism as developed earlier and then introduce the procedure to extend it to finite  $\mu_q$  and  $\mu_c$ . In Sec. III, we calculate and discuss the results of susceptibilities, using the light-light sector to constrain the  $\mu_B$ -dependent potential parameters, and then focus on the heavy-light susceptibilities and their interpretation in the context of IQCD data. In Sec. IV, we conclude and indicate future lines of investigation.

## II. $T$ -MATRIX FORMALISM AT FINITE CHEMICAL POTENTIAL

The theoretical framework used in this work is thermodynamic  $T$  matrix developed in Refs. [23,24] for the quark-gluon plasma. It is based on a Dyson-Schwinger type setup for in-medium one- and two-body propagators, where the scattering kernel is approximated through a three-dimensional (3D) reduction of the 4D Bethe-Salpeter

equation. This enables closed-form solutions and facilitates constraints of the in-medium potential through IQCD data for the HQ free energy. For the “strongly coupled scenario” (SCS), which we will focus on here, the in-medium potential is significantly larger than the free energy, with long-range remnants of the confining force surviving well above  $T_{pc}$ , where they play a central role for the long-wavelength properties of the QGP (such as transport coefficients).

Let us briefly review the relevant ingredients employed in our previous papers [23,24]. Progress in our previous papers essential to this work is that we have developed a method that can evaluate the grand potential (negative pressure) nonperturbatively, where bound-state contributions to the pressure can be included dynamically. This method lends itself to extending the calculation of the pressure to finite chemical potential and then taking the relevant derivatives to obtain the susceptibilities. The method is based on the Luttinger-Ward formalism [45], within which the grand potential (or negative pressure,  $\Omega = -P$ ) in the  $T$ -matrix approach has been formulated as

$$\Omega = \mp \sum \text{Tr} \{ \ln(-G^{-1}) + [(G^0)^{-1} - G^{-1}]G \} \pm \Phi, \quad (1)$$

where  $G^0$  are “bare” parton propagators and  $G = ([G^0]^{-1} - \Sigma)^{-1}$  is the corresponding dressed propagator with self-energy  $\Sigma$  encoding the medium modifications. The first two terms are commonly associated with the one-particle contribution to the pressure, while the Luttinger-Ward functional (LWF),  $\Phi$ , encodes the contribution from the correlated many-body physics. In particular, the LWF can account for the physics of dynamically generated bound states if the  $t$ -channel ladder diagrams with an extra factor  $1/\nu$  are resummed as

$$\Phi = \frac{1}{2} \sum \text{Tr} \left\{ G \left[ V + \frac{1}{2} V G_{(2)}^0 V + \dots + \frac{1}{\nu} V G_{(2)}^0 V G_{(2)}^0 \dots V + \dots \right] G \right\} \quad (2)$$

$$= -\frac{1}{2} \ln [1 - V G_{(2)}^0]. \quad (3)$$

The two-particle propagator,  $G_{(2)}^0$ , is defined as  $G_{(2)}^0 = -\beta^{-1} \sum_{\omega_n} G(iE_n - \omega_n) G(-i\omega_n)$ , which is the energy convolution of two dressed one-particle propagators  $G$ . The  $V$  in the above equation is the interaction kernel, which is the two-body potential in this framework. The  $1/\nu$  factor in Eq. (3) renders the resummation nontrivial, for which a matrix-log method [third line of Eq. (3)] has been developed in Ref. [23,24] to overcome this difficulty. The self-consistent self-energy  $\Sigma$  should be a functional derivative of the LWF  $\delta\Phi/\delta G = \Sigma$  [46,47]. Taking this derivative with the expression in Eq. (3), we obtain the self-energy schematically expressed via the  $T$ -matrix as

$$\Sigma = \int d\tilde{p} T G, \quad T = V + V G_{(2)}^0 T. \quad (4)$$

The  $T$ -matrix equation is an integral equation that resums the ladder diagrams without the  $1/\nu$  factor, and also includes the physics of bound states matching those in the LWF. The above

two equations (4) form a self-consistency problem, which we have solved through numerical iterations.

To calculate susceptibilities, we need to extend the  $T$ -matrix formalism to finite chemical potentials. In this work, we focus on the light-quark ( $\mu_q$ ) and charm-quark ( $\mu_c$ ) chemical potentials. The pertinent dependencies need to be added to the propagators and the two-body potential,  $V$ , which are the two most important components of the  $T$ -matrix approach. At a finite  $\mu_q$  and  $\mu_c$ , the “bare” quark propagators take the form

$$G_i^0(z, \mathbf{p}) = \frac{1}{z - \varepsilon_p \pm \mu_i}, \quad \varepsilon_p = \sqrt{M_i^2 + p^2} \quad (5)$$

with  $i = q, c$  for light or charm quarks, respectively. For simplicity, the strange quark is treated as a light flavor degenerate with  $u$  and  $d$  quarks. The gluon propagator does not have an explicit  $\mu_i$  dependence. However, for all effective thermal-parton masses,  $M_i$ , we allow for an additional  $\mu_q$  dependence as

$$M_i = M_i^0 \sqrt{1 + b_m \left(\frac{\mu_q}{T}\right)^2} + M_i^V, \quad (6)$$

where the  $M_i^0$  denote temperature-dependent perturbative masses at  $\mu_q = 0$  which are adjusted in Ref. [24] by fitting the QGP EoS from lattice QCD. The functional form of the  $\mu_q$  dependence of the masses is motivated by HTL calculations at finite chemical potential [48]; in practice, we will be able to fix the parameter  $b_m$  close to its perturbative value of  $1/\pi^2$  (for  $N_f = N_c = 3$ ) while fitting the baryon number susceptibility,  $\chi_2^B$ , computed in IQCD [27,28], via a temperature-dependent parameter  $b_s$  in the Debye mass [see Eq. (8) below] to encode nonperturbative effects in the potential screening. The  $M_i^V$  mass terms are self-consistently generated from the infinite-distance limit of the in-medium potential as discussed in Ref. [24]. They will acquire an intrinsic  $\mu_q$  dependence through the potential depending on  $\mu_q$ .

For the two-body potential,  $V$ , figuring in Eq. (3) and the  $T$  matrix, we keep the form introduced in Ref. [24], which is evaluated in momentum space and dressed with relativistic corrections. In coordinate space and in the static limit, and with the constant term  $-(4/3)\alpha_s m_d + \sigma/m_s$  subtracted, it is given by

$$V(r) = -\frac{4}{3}\alpha_s \frac{e^{-m_d r}}{r} + \sigma \frac{e^{-m_s r - (c_b m_s r)^2}}{m_s}. \quad (7)$$

The parameters of the potential are taken from the strongly coupled solution (SCS) in Ref. [24]. The only addition here is a  $\mu_q$  dependence to the original Debye screening mass by using the ansatz

$$m_d = m_d^0 \sqrt{1 + b_s \left(\frac{\mu_q}{T}\right)^2}, \quad (8)$$

where  $m_d^0$  is the  $T$ -dependent zero-chemical potential value fixed in Ref. [24] essentially in fits to the HQ free energy. Also this ansatz is motivated by the HTL results of Ref. [48] with  $b_s$  being our second parameter in fitting to  $\chi_2^B$  [28]. Note that the screening of the string term is not independent but will be determined by  $m_d$  according to the relation  $m_s \propto (\sigma m_d^2)^{1/4}$ ; cf. Sec. III D 1 of Ref. [24].

With the additional ingredients specified in the three equations above, the  $T$ -matrix approach is generalized to finite chemical potential. We first self-consistently evaluate the coupled system of Dyson-Schwinger equations for the single-parton propagators and their two-body  $T$ -matrices in all available color channels and up to  $L = 5$  partial waves. Then, using the same procedure as in our original work [24], the pressure,  $P(\mu_q, \mu_c)$ , can be calculated as a function of  $\mu_q$  and  $\mu_c$  using the matrix-log resummation technique for the Luttinger-Ward functional introduced in Refs. [23,24]. We define the dimensionless pressure as  $\hat{P}(\hat{\mu}_q, \hat{\mu}_c) = P(\hat{\mu}_q T, \hat{\mu}_c T)/T^4$ , where the  $\hat{\mu}_i = \mu_i/T$  are also dimensionless. The susceptibilities are obtained from the numerical derivatives of the pressure  $\hat{P}$  with respect to  $\hat{\mu}_q$  and  $\hat{\mu}_c$ . Since  $\mu_q = (1/3)\mu_B$ , the second-order baryon number susceptibility follows from quark-number susceptibility as

$$\chi_2^B = \frac{\partial^2 \hat{P}}{\partial \hat{\mu}_B^2} = \frac{1}{9} \frac{\partial^2 \hat{P}}{\partial \hat{\mu}_q^2}. \quad (9)$$

Likewise, we obtain the off-diagonal heavy-light susceptibilities as

$$\chi_{nm}^{qc} = \frac{\partial^{n+m} \hat{P}}{\partial \hat{\mu}_q^n \partial \hat{\mu}_c^m}. \quad (10)$$

In Ref. [33],  $\chi_{nm}^{uc}$  is explicitly shown (rather than  $\chi_{nm}^{qc}$ ). Since the  $u, d$ , and  $s$  quarks are treated as degenerate in our work, we have for the case  $n = 1$  the relation

$$\chi_{1m}^{uc} = \frac{\partial^{1+m} \hat{P}}{\partial \hat{\mu}_u \partial \hat{\mu}_c^m} = \frac{1}{3} \frac{\partial^{1+m} \hat{P}}{\partial \hat{\mu}_q \partial \hat{\mu}_c^m}. \quad (11)$$

For  $n = 2$ , we have the approximate relation

$$\chi_{2m}^{uc} = \frac{\partial^{2+m} \hat{P}}{\partial \hat{\mu}_u \partial \hat{\mu}_c^m} \approx \frac{1}{3} \frac{\partial^{2+m} \hat{P}}{\partial \hat{\mu}_q^2 \partial \hat{\mu}_c^m}, \quad (12)$$

where we neglect small terms like  $\chi_{11m}^{udc}, \chi_{11m}^{usc}, \chi_{11m}^{dsc}$ . Using  $\chi_{mn}^{BC}$  data from Ref. [33] we have verified that these terms lead to less than 20% difference at  $T = 0.194$  GeV (the lowest  $T$  in our work), and that they are negligible at higher temperature.

### III. NUMERICAL RESULTS

In our numerical evaluation of the chemical-potential derivatives, we start by self-consistently evaluating the pressure,  $\hat{P}(\hat{\mu}_q, \hat{\mu}_c)$ , on a grid of 12 pairs of values for the light- and charm-quark chemical potentials (all combinations of  $\hat{\mu}_q = 0, 0.2$  and  $\hat{\mu}_c = 0.2, 0.4, 0.6, 0.8$ ), for a given input of the  $b_m$  and  $b_s$  parameters (we work in a “quenched-charm” approximation as was done in the IQCD computations of Ref. [33], where charm quarks are not part of the bulk medium). Utilizing a polynomial ansatz for the pressure,

$$\begin{aligned} \hat{P}(\mu_q, \mu_c) = & \hat{P}_0 + \frac{\chi_2^q}{2} \hat{\mu}_q^2 + \frac{\chi_2^c}{2} \hat{\mu}_c^2 + \frac{\chi_4^c}{4!} \hat{\mu}_c^4 \\ & + \frac{\chi_{11}^{uc}}{1!1!} \hat{\mu}_q \hat{\mu}_c + \frac{\chi_{22}^{uc}}{2!2!} \hat{\mu}_q^2 \hat{\mu}_c^2 + \frac{\chi_{13}^{uc}}{1!3!} \hat{\mu}_q \hat{\mu}_c^3 \end{aligned} \quad (13)$$

(where  $\hat{P}_0$  denotes the scaled pressure at vanishing chemical potentials), we fit its coefficients to the numerically computed

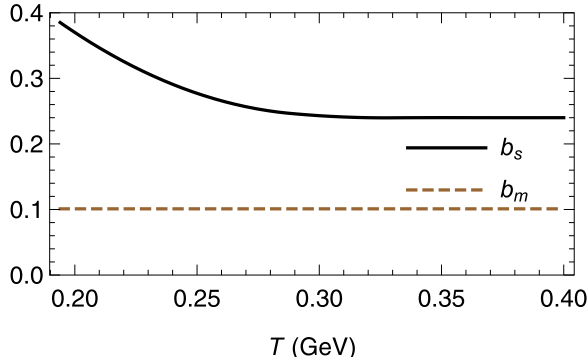


FIG. 1. Results for the temperature dependence of the parameters  $b_s$  and  $b_m$  (introducing a  $\mu_q$  dependence for the screening mass in the potential and for the thermal parton masses in the EoS, respectively) following from the fit shown in the upper panel of Fig. 2.

results from the  $T$ -matrix approach. Note that the susceptibilities defined by the derivatives to the pressure are also the coefficients of its Taylor expansion in terms of  $\mu_q$  and  $\mu_c$ . The fits are truncated at fourth order in  $\hat{\mu}_c$  and second order in  $\hat{\mu}_q$ , corresponding to the minimal orders required to extract the susceptibilities considered in this work. The  $\hat{\mu}_q$  value is chosen sufficiently small as to render higher orders negligible, while the relatively large upper value of  $\hat{\mu}_c$  is required to generate sufficient sensitivity to the response in charm-quark fluctuations.

We first tune the parameters  $b_m$  and  $b_s$  to reproduce the baryon-number susceptibility,  $\chi_2^B(T)$ , computed on the lattice (where  $\hat{\mu}_c$  is set to zero). Note that in our definition  $\chi_2^B$  is dimensionless (corresponding to  $\chi_2^B/T^2$  in the convention where pressure and chemical potentials are not scaled by powers of temperature). As we mentioned above, it turns out that we can fix the  $b_m$  parameter, which characterizes the  $\mu_q$  dependence of the effective parton masses, at the perturbative value of  $1/\pi^2$ , while introducing a temperature dependence into  $b_s$  to allow for nonperturbative screening effects [48]. The magnitude of  $b_s$  turns out to be significantly larger than its perturbative value (which is also  $1/\pi^2$ ), especially when approaching  $T_{pc}$  from above; see Fig. 1 (and the resulting baryon susceptibility in the upper panel of Fig. 2). This suggests that at the highest temperature considered here,  $T = 400$  MeV, nonperturbative effects in the  $\mu_q$  dependence of the potential are still significant, which may not be surprising as the potential itself still carries significant contributions from the string interactions (see also Fig. 3 below). We have geared our fit of  $\chi_2^B$  toward the IQCD data of the Hot-QCD Collaboration [28] (denoted as “lat1”), since their results were the basis for our self-consistent fits of the EoS in our previous work [24]. The IQCD data for  $\chi_2^B$  from the Wuppertal-Budapest group [27] (denoted by “lat2”) are somewhat smaller.

The resulting  $\mu_q$  dependence of the two-body potential is displayed in Fig. 3. Since the density of the partons in the medium increases with  $\mu_q$ , the potential exhibits an expected increase in screening at fixed temperature. However, this effect appears to be relatively moderate: e.g., at  $\mu_q/T = 1$ , the increase in  $m_d$  amounts to only  $\approx 10$ – $20$  %. Recalling the relation between the color-Coulomb Debye mass

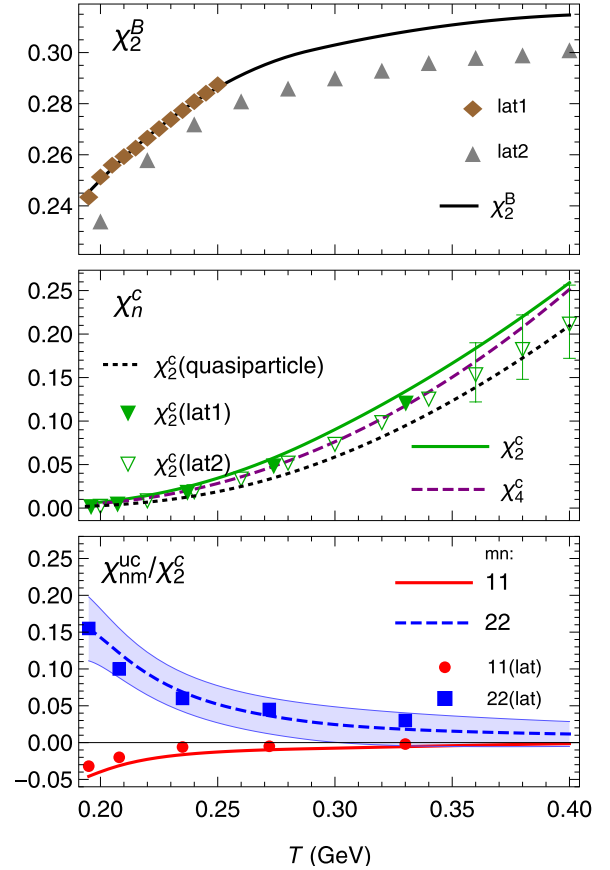


FIG. 2. Upper panel: our fit to the baryon susceptibility,  $\chi_2^B$ , of the IQCD data by the Hot-QCD Collaboration (“lat1”) [28]; also shown are the results of the Wuppertal-Budapest group (“lat2”) [27]. Middle panel: our predictions for the diagonal charm susceptibilities  $\chi_2^c$  (solid line) and  $\chi_4^c$  (dashed line), compared to  $N_f = 2 + 1$  Hot-QCD and  $N_f = 2 + 1 + 1$  Wuppertal-Budapest IQCD data; also shown is our result when neglecting charm-quark widths and heavy-light correlations (dotted line). Lower panel: heavy-light susceptibilities  $\chi_{nm}^{uc}/\chi_2^c$  with  $1\sigma$  error band compared to Hot-QCD IQCD data [33].

and the screening mass of the string term,  $m_s \propto (\sigma m_d^2)^{1/4}$ , and the infinite-distance value of the potential,  $V(r = \infty) = -(4/3)\alpha_s m_d + \sigma/m_s$  [24], we find that the long-range part of the potential is only suppressed by  $\approx 5$ – $10$  %. While the predominant impact of the finite chemical potential originates from the parton propagators, Eq. (5), the additional  $\mu_q$  dependence of the potential and quark masses is essential to achieve a good fit to  $\chi_2^B$ . This indicates that the quark number susceptibilities are sensitive to microscopic physics at finite  $\mu_B$ .

Next, we turn to the diagonal charm susceptibilities,  $\chi_2^c$  and  $\chi_4^c$ , shown in the middle panel of Fig. 2. Since they are essentially independent of  $\mu_q$ , they are genuine predictions of the  $T$ -matrix calculations at  $\mu_q = 0$  where all parameters were fixed in our previous work [24]. The result for  $\chi_2^c$  shows good agreement with the Hot-QCD lattice results, while the Wuppertal-Bielefeld results are somewhat lower (we recall that the latter have been computed in  $N_f = 2 + 1 + 1$  flavor QCD, i.e., including dynamical charm quarks, while our

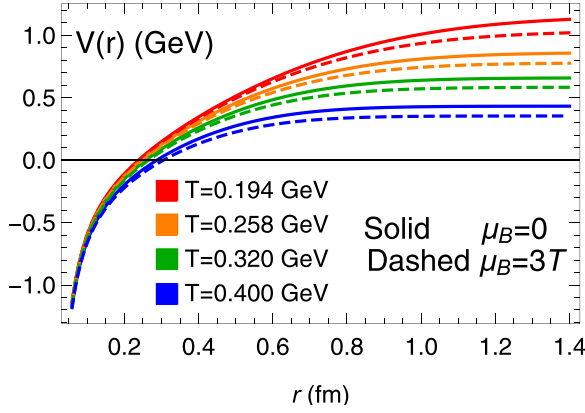


FIG. 3. The effects of the finite- $\mu_q$  screening on the in-medium two-body potential in the color-singlet channel resulting from our fit to the baryon susceptibility,  $\chi_2^B$  (solid lines:  $\mu_q = 0$ ; dashed lines:  $\mu_q = T$ ).

results are closer to the quenched-charm approximation as adopted in the Hot-QCD computations). In particular, the  $T$ -matrix results are significantly larger than calculations using a quasiparticle approximation with the same charm-quark pole mass as in the  $T$  matrix; in other words, the finite-width effects in the charm-quark spectral functions (with  $\Gamma_c \simeq 0.5$  GeV) and the interaction effects in the Luttinger-Ward functional of the pressure (including broad  $D$ -meson and heavy-light diquark bound states for temperatures below  $T \simeq 250$  MeV) are essential for the agreement with the IQCD data. In view of this, it appears rather nontrivial that also the fourth-order derivative is in approximate agreement with the IQCD data, which exhibit a close agreement between  $\chi_2^c$  and  $\chi_4^c$  (we have also verified that residual numerical uncertainties are rather significant in our extraction of  $\chi_4^c$ : e.g., when reducing the numerical tolerance from 5 to 4 digit accuracy,  $\chi_4^c$  is reduced by ca. 10% toward higher temperatures).

Finally, we turn to the off-diagonal susceptibilities, which are commonly normalized by  $\chi_2^c$  to achieve a (partial) cancellation of the HQ mass effects. It turns out that the fit of the  $\chi$  coefficients to the pressure, Eq. (13), which we have numerically computed on a finite number of mesh points in the  $\hat{\mu}_q$ - $\hat{\mu}_c$  plane, allows for several minima where the deviations between fitted and calculated data are of order  $10^{-5}$  or below. Since this is small compared to our current numerical accuracy, the different minima are *a priori* equally likely to represent the “true” solution. To lift this degeneracy, we therefore impose a constraint,  $\chi_{13}^{uc} = \chi_{11}^{uc}$ , motivated by IQCD data (and related to the expectation that the contribution of particles with charm-number larger than 1 is negligible) [32], to find the minimum compatible with this condition (in principle, we could then release it again and find a local minimum with  $\chi_{13}^{uc} \approx \chi_{11}^{uc}$ , but for simplicity we focus on the results with the constraint  $\chi_{13}^{uc} = \chi_{11}^{uc}$ ). We reiterate that we have not “refit” the two “b” parameters which were solely fixed through the light-quark susceptibilities (cf. the second paragraph in Sec. II). Therefore, the resulting heavy-light susceptibilities can also be regarded as predictions of the model, with the numerical caveat outlined above. The pertinent results are shown in the lower panel of Fig. 2 in terms of  $\chi_{11}^{uc}/\chi_2^c$  and  $\chi_{22}^{uc}/\chi_2^c$ , where

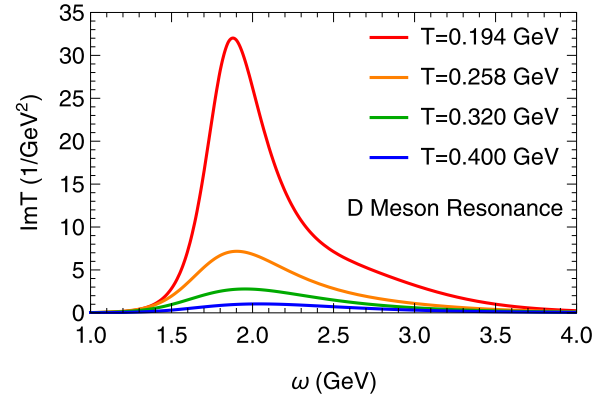


FIG. 4. The imaginary part of the charm-light quark  $T$ -matrix in the  $S$ -wave color-singlet channel at four temperatures. One recognizes the emergence of  $D$ -meson-like resonance as the temperature approaches  $T_{pc}$  from above.

the error band illustrates the  $1\sigma$  band of the fit, indicating that the extraction of  $\chi_{22}^{uc}$  (and other fourth-order coefficients) is rather challenging in this calculation (the uncertainty is much smaller for  $\chi_{11}^{uc}$ ). Again, we find a fair semiquantitative agreement with IQCD data, which generally supports the role of nonperturbative physics in the QGP near  $T_{pc}$ . The strongly coupled features of the system, such as large scattering rates of the partons (which suppress the single-parton contributions) and the related onset of heavy-light bound-state formation (which enhance the correlated parton contributions, cf. Fig. 4) do not lead to apparent discrepancies with charm-quark susceptibilities computed in IQCD. The only other calculation we are aware of is a mean-field hadron-quark crossover model which predicts a positive  $\chi_{11}^{uc}$  [39], while the  $\chi_{11}^{us}$  calculated in that work is negative and in agreement with IQCD data, thus we find no obvious connection between those two quantities. On the other hand, the HTL perturbative analysis of Ref. [34] finds vanishing off-diagonal  $us$  and  $ud$  susceptibilities while in the PNJL calculations of Refs. [36,37] the results for  $\chi_{11}^{us}$  are negative but tend to underpredict the IQCD data; in particular, fluctuations beyond the mean-field level were found to be essential to improve the agreement with IQCD data [36]. In a very recent HRG analysis [38], the inclusion of an extended set of strange-baryon resonances as predicted by the quark model, in combination with excluded-volume corrections, can reproduce the IQCD results up to  $T \simeq 170$  MeV, where the interplay of mesonic and baryonic contribution, which have opposite signs [36], is critical. Our calculations also include such effects through the dynamical formation of mesonic and diquark resonances in the attractive color channels (color singlet and antitriplet, respectively; cf. Fig. 4). However, the resonance correlations dissolve as temperature increases, which is essential for the agreement with IQCD data at higher temperature.

We have also attempted to calculate the heavy-light susceptibilities using the “weakly coupled solution” (WCS) of Ref. [24] (where the interquark potential is close to the HQ free energy); however, the results were quantitatively rather inconclusive (i.e., numerically unstable) due to the sharp spectral functions (with small widths) in the parton propagators,

which compromises the numerical accuracy. Nevertheless, the sign of  $\chi_{22}^{uc}/\chi_2^c$  appears to turn negative at low temperature;  $\chi_{11}^{uc}/\chi_2^c$  is more stable and of the same sign as in the SCS plotted in Fig. 2, albeit of smaller magnitude. Further scrutiny of this finding is in order to better establish the degree to which heavy-light susceptibilities are sensitive to the underlying color forces.

#### IV. CONCLUSIONS AND PERSPECTIVE

Employing a thermodynamic  $T$ -matrix approach to the QGP extended to finite chemical potential, we have performed calculations of various quark-number susceptibilities in a strongly coupled scenario. Toward this end we have introduced two additional model parameters into our framework which quantify the leading order corrections in  $\mu_q$  to the screening mass of the interaction kernel and the bare light-parton masses of the bulk medium. They have been fit to reproduce the temperature dependence of the IQCD data for the second-order baryon susceptibility,  $\chi_2^B$ . The additional screening of the in-medium potential at finite  $\mu_q$  turns out to be rather moderate. The resulting diagonal charm-quark susceptibilities,  $\chi_2^c$  and  $\chi_4^c$ , which do not depend on the additional fit parameters and thus can be considered predictions of our approach, show fair agreement with the IQCD results. In particular, the large collisional widths inherent in the charm-quark spectral functions, as well as bound-state correlations close to  $T_{pc}$ , are instrumental in this agreement (as demonstrated by a calculation with quasiparticle charm quarks, which falls short of the IQCD data). We have also computed the off-diagonal charm susceptibilities,  $\chi_{11}^{uc}/\chi_2^c$  and  $\chi_{22}^{uc}/\chi_2^c$ , for which very few results exist in the literature. Our calculations lead to fair agreement with pertinent IQCD data; most notably, when approaching  $T_{pc}$  from above, we find increasingly negative values of  $\chi_{11}^{uc}/\chi_2^c$ , which to our knowledge has not been reported before in a microscopic

model approach. Our findings imply that a strongly coupled system where large collisional widths are driven by the emergence of near-threshold resonances in attractive heavy-light color channels and produce a small HQ diffusion coefficient,  $2\pi TD_s \simeq 2-5$  [23], remains a viable realization of the sQGP at moderate temperatures.

Several future developments are in order to further scrutinize our understanding of these mechanisms. The current  $T$ -matrix formalism only accounts for mesonic and diquark channels; while the latter is a building block of baryons, the inclusion of genuine three-body interactions remains to be elaborated, which is particularly interesting in view of charm-baryon production in nuclear collisions at the Large Hadron Collider and its implementation in recombination models [44]. Furthermore, the effects of spin-spin and spin-orbit interactions should be studied; they are dictated by a quantitative hadron spectroscopy in vacuum and are presumably essential to construct a smooth cross-over from partonic to hadronic bulk matter. Finally, the development in the present paper paves the way for deploying the  $T$ -matrix formalism into the finite- $\mu_q$  plane of the QCD phase diagram, where it could help us to understand the microscopic interactions underlying the transport and spectral properties of QCD matter as produced in heavy-ion collisions at lower energies and in neutron stars and their mergers. Work in some of these directions is in progress.

#### ACKNOWLEDGMENTS

This work was supported by the Strategic Priority Research Program of Chinese Academy of Sciences, Grant No. XDB34000000 and Fundamental Research Funds for the Central Universities (S.Y.F.L.), and by the U.S. National Science Foundation (NSF) through Grants No. PHY-1913286 and No. PHY-2209335 (R.R.).

- 
- [1] E. Shuryak, *Rev. Mod. Phys.* **89**, 035001 (2017).
  - [2] P. Braun-Munzinger, V. Koch, T. Schäfer, and J. Stachel, *Phys. Rep.* **621**, 76 (2016).
  - [3] W. Busza, K. Rajagopal, and W. van der Schee, *Annu. Rev. Nucl. Part. Sci.* **68**, 339 (2018).
  - [4] X. Dong, Y.-J. Lee, and R. Rapp, *Annu. Rev. Nucl. Part. Sci.* **69**, 417 (2019).
  - [5] S. Borsanyi, G. Endrodi, Z. Fodor, A. Jakovac, S. D. Katz, S. Krieg, C. Ratti, and K. K. Szabo, *J. High Energy Phys.* **11** (2010) 077.
  - [6] A. Bazavov *et al.* (HotQCD Collaboration), *Phys. Rev. D* **90**, 094503 (2014).
  - [7] Y. Aoki, G. Endrodi, Z. Fodor, S. D. Katz, and K. K. Szabo, *Nature (London)* **443**, 675 (2006).
  - [8] P. Levai and U. W. Heinz, *Phys. Rev. C* **57**, 1879 (1998).
  - [9] A. Peshier and W. Cassing, *Phys. Rev. Lett.* **94**, 172301 (2005).
  - [10] S. Plumari, W. M. Alberico, V. Greco, and C. Ratti, *Phys. Rev. D* **84**, 094004 (2011).
  - [11] C.-Y. Wong, *Phys. Rev. C* **72**, 034906 (2005).
  - [12] A. Mocsy and P. Petreczky, *Phys. Rev. D* **73**, 074007 (2006).
  - [13] D. Cabrera and R. Rapp, *Phys. Rev. D* **76**, 114506 (2007).
  - [14] W. M. Alberico, A. Beraudo, A. De Pace, and A. Molinari, *Phys. Rev. D* **75**, 074009 (2007).
  - [15] A. Mocsy and P. Petreczky, *Phys. Rev. D* **77**, 014501 (2008).
  - [16] F. Riek and R. Rapp, *New J. Phys.* **13**, 045007 (2011).
  - [17] S. Y. F. Liu and R. Rapp, *Nucl. Phys. A* **941**, 179 (2015).
  - [18] A. Rothkopf, *Phys. Rep.* **858**, 1 (2020).
  - [19] G. Aarts, C. Allton, M. B. Oktay, M. Peardon, and J.-I. Skullerud, *Phys. Rev. D* **76**, 094513 (2007).
  - [20] G. Aarts, C. Allton, S. Kim, M. P. Lombardo, M. B. Oktay, S. M. Ryan, D. K. Sinclair, and J. I. Skullerud, *J. High Energy Phys.* **11** (2011) 103.
  - [21] P. Petreczky and K. Petrov, *Phys. Rev. D* **70**, 054503 (2004).
  - [22] O. Kaczmarek and F. Zantow, *Phys. Rev. D* **71**, 114510 (2005).
  - [23] S. Y. F. Liu and R. Rapp, *Eur. Phys. J. A* **56**, 44 (2020).
  - [24] S. Y. F. Liu and R. Rapp, *Phys. Rev. C* **97**, 034918 (2018).
  - [25] S. Y. F. Liu, M. He, and R. Rapp, *Phys. Rev. C* **99**, 055201 (2019).
  - [26] S. Y. F. Liu and R. Rapp, *J. High Energy Phys.* **08** (2020) 168.

- [27] S. Borsanyi, Z. Fodor, S. D. Katz, S. Krieg, C. Ratti, and K. Szabo, *J. High Energy Phys.* **01** (2012) 138.
- [28] A. Bazavov *et al.* (HotQCD Collaboration), *Phys. Rev. D* **86**, 034509 (2012).
- [29] R. Bellwied, S. Borsanyi, Z. Fodor, S. D. Katz, A. Pasztor, C. Ratti, and K. K. Szabo, *Phys. Rev. D* **92**, 114505 (2015).
- [30] H. T. Ding, S. Mukherjee, H. Ohno, P. Petreczky, and H. P. Schadler, *Phys. Rev. D* **92**, 074043 (2015).
- [31] C. Ratti, *Rep. Prog. Phys.* **81**, 084301 (2018).
- [32] A. Bazavov *et al.*, *Phys. Lett. B* **737**, 210 (2014).
- [33] S. Mukherjee, P. Petreczky, and S. Sharma, *Phys. Rev. D* **93**, 014502 (2016).
- [34] N. Haque, A. Bandyopadhyay, J. O. Andersen, M. G. Mustafa, M. Strickland, and N. Su, *J. High Energy Phys.* **05** (2014) 027.
- [35] J. P. Blaizot, E. Iancu, and A. Rebhan, *Phys. Lett. B* **523**, 143 (2001).
- [36] C. Ratti, R. Bellwied, M. Cristoforetti, and M. Barbaro, *Phys. Rev. D* **85**, 014004 (2012).
- [37] A. Bhattacharyya, S. K. Ghosh, S. Maity, S. Raha, R. Ray, K. Saha, and S. Upadhaya, *Phys. Rev. D* **95**, 054005 (2017).
- [38] J. M. Karthein, V. Koch, C. Ratti, and V. Vovchenko, *Phys. Rev. D* **104**, 094009 (2021).
- [39] A. Miyahara, M. Ishii, H. Kouno, and M. Yahiro, *Int. J. Mod. Phys. A* **32**, 1750205 (2017).
- [40] H. van Hees and R. Rapp, *Phys. Rev. C* **71**, 034907 (2005).
- [41] H. van Hees, M. Mannarelli, V. Greco, and R. Rapp, *Phys. Rev. Lett.* **100**, 192301 (2008).
- [42] F. Riek and R. Rapp, *Phys. Rev. C* **82**, 035201 (2010).
- [43] A. Beraudo *et al.*, *Nucl. Phys. A* **979**, 21 (2018).
- [44] M. He and R. Rapp, *Phys. Rev. Lett.* **124**, 042301 (2020).
- [45] J. M. Luttinger and J. C. Ward, *Phys. Rev.* **118**, 1417 (1960).
- [46] G. Baym and L. P. Kadanoff, *Phys. Rev.* **124**, 287 (1961).
- [47] G. Baym, *Phys. Rev.* **127**, 1391 (1962).
- [48] J. P. Blaizot, E. Iancu, and A. Rebhan, *Phys. Lett. B* **470**, 181 (1999).